ANALYTICAL SCIENCES NOVEMBER 2019, VOL. 35

An Electrochemical Sensor Based on Structure Switching of Dithiol-modified Aptamer for Simple Detection of Ochratoxin A

Donny Nugraha MAZAAFRIANTO,[*1] **Akihiko ISHIDA,**[*2†] **Masatoshi MAEKI,**[*2] **Hirofumi TANI,**[*2] **and Manabu TOKESHI**[*2,*3,*4,*5†]

*1 *Graduate School of Chemical Sciences and Engineering, Hokkaido University, Japan*
*2 *Division of Applied Chemistry, Faculty of Engineering, Hokkaido University, Japan*
*3 *ImPACT Research Center for Advanced Nanobiodevices, Nagoya University, Japan*
*4 *Innovative Research Center for Preventive Medical Engineering, Nagoya University, Japan*
*5 *Institute of Innovation for Future Society, Nagoya University, Japan*

In this study, we developed an electrochemical sensor for ochratoxin A (OTA) by using an aptamer having a dithiol-based anchor, which exhibited higher stability on a gold electrode than a monothiol-based aptamer because of its two anchors. The sensor was also based on a signal-on scheme that produces a signal current resulting from structure-switching of the aptamer upon interaction with OTA. For simple fabrication of this sensor, the non-covalent interaction of methylene blue with the aptamer was also employed as an electrochemical indicator. In this study, the performance of the sensor, including the dissociation constant of the aptamer–OTA complex, was characterized. The proposed sensor exhibited high reproducibility and enough sensitivity to detect the minimum amount of OTA required for the analysis of real food samples with a limit of detection of 113 pM.

Keywords Dithiol, microfabricated device, electrochemical detection, aptamer, methylene blue, ochratoxin A, signal-on

(Received June 26, 2019; Accepted July 8, 2019; Advance Publication Released Online by J-STAGE July 19, 2019)

Introduction

Recently, the detection of pathogens and food contaminants in the quality control of food products has attracted special attention. Although many analytical techniques, including chromatography,[1,2] spectroscopy,[3,4] and quartz crystal microbalance[5,6] have been employed for this detection, electrochemical techniques exhibit great promise owing to high sensitivity, low cost, and simplicity in instrumentation and operation.[7–11] For mycotoxins, several electrochemical sensors have been designed using aptamers, which are in an emerging class of biorecognition molecules that can potentially replace antibodies. This type of molecule involves nucleic acid ligands that are isolated from a random sequence of DNA pools by systematic evolution of ligands by the exponential enrichment (SELEX). Aptamers bind tightly to targets with high specificity, which is characterized with dissociation constants (K_d) in the micromolar to nanomolar range.[12,13]

In aptamer-based sensors, aptamers were modified with labels, such as a redox compound, fluorescent dye, and enzyme.[14–16] Ferrocene and methylene blue (MB) have been commonly used as redox reporters owing to their electrochemically reversible behavior. Moreover, the differences in the performances of the above redox reporters have been investigated. González-Fernández *et al.* reported that MB provides a stable background and reproducible responses, compared to ferrocene.[17] Moreover, the ability of MB to interact with the guanine bases of DNA *via* π–π interactions has been reported.[11,18] Therefore, MB has emerged advantageous as a redox label.[19–22] Besides redox labels, several strategies have been studied to enhance the sensitivity of detection with metal nanoparticles, carbon nanotubes, and magnetic beads.[10,23,24] Although the high sensitivity and short analysis time of the sensors have been highlighted, most sensors were constructed in complex multi-preprocessing steps with covalently labeled aptamers. Thus, such sensors required special treatment in each fabrication step.

For electrochemical aptamer sensors, there have been several reports on a detection scheme based on the structure switching of aptamers,[11,14,29] which causes the target-induced dissociation (TID) of the aptamer from the sensor surface and produces a decreased signal (switch-off scheme). However, TID-based sensors might provide positive errors because external factors might dissociate the aptamer.

The increase in the stability of immobilized aptamers on the gold electrode also presented a challenge in obtaining reproducible results. Several investigations, including our preliminary study, suggested that the self-assembled layers comprising monothiol-based aptamers were unstable on the gold surface. Liepold *et al.* reported that the layer of a thiol-anchoring compound formed on a gold surface was subjected to a "stress condition" by adding another thiol-containing compound, which displaced the initially immobilized thiol compound.[25] The monothiol-based aptamer was displaced with another thiol compound, such as 6-mercaptohexanol (MCH), typically used for avoiding unspecific bonding to the remaining

† To whom correspondence should be addressed.
E-mail: ishida-a@eng.hokudai.ac.jp (A. I.); tokeshi@eng.hokudai.ac.jp (M. T.)

gold sites, which resulted in an irreproducible decrease in the signal.[25,26] However, increasing the number of thiol groups of the anchoring sites of the aptamer can enable much stronger interaction with the gold surface, and hence, the sensor can provide reproducible signals. In fact, several studies have revealed that dithiol-modified DNAs bind more strongly to the gold surface than monothiol ones.[25,27]

In this study, we have developed a reliable electrochemical sensor having three key features: First, an aptamer having a dithiol anchor was used to obtain reproducible signals by avoiding the replacement of the aptamer with MCH, as described above. Second, the problem of TID-detection schemes was addressed by employing a signal-on detection scheme, which was based on structure switching of the aptamer upon interaction with the target compound. Thus, in the proposed sensor, the addition of the target to the sensor triggers the structure switching, producing a signal current (switch-on scheme). Third, for a simple construction of the sensor, we also used non-covalently labeled MB as a redox probe, which interacts with the aptamer through guanine bases. To the best of our knowledge, there is no report on such an electrochemical sensor. The performance of the proposed sensor is evaluated using ochratoxin A (OTA), which is potentially carcinogenic to humans and frequently found in food and beverage products.

Experimental

Materials and reagents

The DNA aptamer was designed according to the literature[28] with some modifications. It contained 36 bases, modified with dithiol phosphoramidite (DTPA) at the 5′-end, incorporated through a 3-carbon spacer (5′-DTPA-C3-GAT CGG GTG TGG GTG GCG TAA AGG GAG CAT CGG ACA-3′), and purified with high-performance liquid chromatography. This aptamer was received as a lyophilized powder from Integrated DNA Technologies (Coralville, USA) and rehydrated by tris–ethylenediaminetetraacetic acid (10 mM Tris–HCl and 1.0 mM EDTA) buffer at a final concentration of 100 μM. The concentration was rechecked using a NanoDrop One/One^C spectrophotometer (Thermo Fisher) to confirm the actual concentration. The buffer solution used for the hybridization and electrochemical measurement was phosphate-buffered saline (PBS, pH 7.2) containing 1 mM $MgCl_2$ (Thermo Fisher). Aflatoxin B1 (AFB1, 2 μg mL^{-1} in acetonitrile, ≥99%) and MCH (≥97%) were procured from Sigma Aldrich. Deoxynivalenol (DON, 99.83 μg mL^{-1} in acetonitrile, ≥99%) was procured from Aokin AG., Germany. MB (≥98.5%), tris-(2-carboxyethyl) phosphine hydrochloride (TCEP, ≥99%), OTA (10 μg mL^{-1} in acetonitrile, ≥99%), and other unspecified chemicals and reagents were of analytical purity and purchased from Wako Pure Chemical Industries, Ltd., Japan. Solutions were prepared with ultrapure water processed with a Milli-Q water purification system (Millipore, 18 MΩ cm at 25°C). A 1.7-mm-thick PS plate (Tamiya Inc., Japan) was used as a substrate for the electrodes.

Fabrication of electrode system on a substrate

The microfabricated electrode system consisted of three thin-film gold electrodes (Fig. S1, Supporting Information). The working electrode had a diameter of d = 5 mm, and the surface of the reference electrode was modified with Ag/AgCl ink. The three-electrode system was fabricated on a PS substrate through gold vacuum deposition and chemical etching. The procedure for the fabrication of the integrated electrode is described in our previous report.[11] Briefly, an Au film was evaporated on two pieces of PS substrates (5 × 5 cm) with a vacuum chamber until a thickness of 1.4 kÅ was achieved. In this process, no adhesive layer between the Au film and PS substrate, such as Cr or Ti layer, was needed. The Au-coated PS substrate was patterned with a photomask by photolithography using an OFPR-800 photoresist (Tokyo Ohka Kogyo Co., Ltd., Japan), and then developed for 1 min in an NMD-3 developer (Tokyo Ohka Kogyo Co., Ltd., Japan). To develop the electrode, the patterned substrate was etched in an I_2/KI solution for 1 min, followed by the removal of the remaining photoresist with isopropyl alcohol. The substrate was soaked in isopropyl alcohol repeatedly until its surface was completely clean. Then, the substrate was rinsed with deionized water and dried with a nitrogen gun. The PS substrate with electrodes was cut into pieces of size 2.5 × 2.5 cm. A small amount of Ag/AgCl ink (ALS Co., Ltd.) was added to the corresponding electrode to form a reference electrode, and then, screws were fixed at the contact pads to connect an electrochemical analyzer. A piece of the PDMS slab with a punched hole (5 mm i.d.) was placed on the substrate to form a well.

Fabrication of electrochemical aptasensor

Aptasensors were constructed on the microfabricated electrode. The procedures for surface treatment prior to the self-assembly of the aptamer monolayer on the gold surface was electrode cleaning, which is very crucial to obtain a smooth surface for immobilization of the aptamer. The electrodes were cleaned by electrochemical oxidation and reduction by repeatedly scanning the potential from –0.35 to –1.35 V *vs.* Ag/AgCl at a scan rate of 2 V s^{-1} in 0.5 M NaOH. Typically, 100 – 200 scans provided a steady-state current. Then, the potential was scanned in 0.5 M H_2SO_4 in the range of –0.35 to 1.5 V *vs.* Ag/AgCl at a scan rate of 0.1 V s^{-1} for 20 scans. A final round of potential scan was performed in 0.1 M H_2SO_4 containing 0.01 M KCl with the following four potential ranges: (1) 0.2 – 0.75 V *vs.* Ag/AgCl, (2) 0.2 – 1.0 V *vs.* Ag/AgCl, (3) 0.2 – 1.25 V *vs.* Ag/AgCl, and (4) 0.2 – 1.5 V *vs.* Ag/AgCl.[11] The entire cleaning process for the microfabricated electrode was conducted in a PDMS well (Figs. S1 and S2, Supporting Information).

Figures 1A – 1C show the schematic diagram of electrode modification with the aptamer, MCH, and MB. Before immobilization, the aptamer was incubated in a 10 mM TCEP solution, followed by dilution with PBS buffer to a final concentration of 1 μM. Then, 50 μL of the diluted solution of the aptamer was transferred to the working electrode and incubated for 60 min. The electrode was thoroughly rinsed with PBS and further passivated with 50 μL of 2 mM MCH in PBS for 60 min to fill the uncovered gold surface. A portion (50 μL) of 20 μM MB solution containing 20 mM KCl was dropped onto the electrode. The PBS buffer was thoroughly flowed over the modified electrode to remove any excess modifier.

Regeneration of the sensor

After sensing OTA with a sensor, the sensing layer was incubated with 50 mM NaOH for 30 min. Afterward, the sensor surface was rinsed with a stream of deionized water and PBS buffer. Then, the sensor was incubated with a 20 μM MB solution (20 mM KCl), and finally, rinsed with PBS buffer (Figs. 1D to 1B).

Electrochemical measurements

All electrochemical experiments were performed with an ALS 1232a electrochemical analyzer (BAS Inc., Japan). Differential

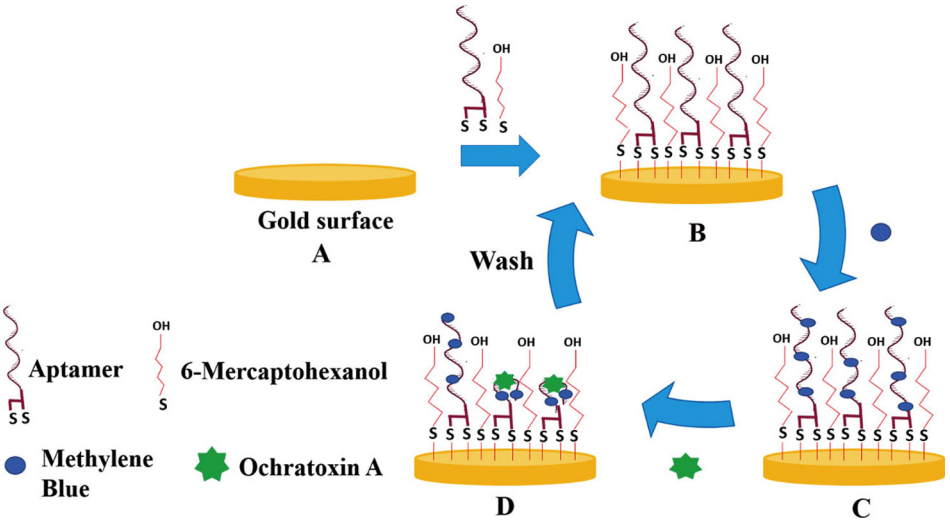

Fig. 1 Schematic of the construction of the sensing layer of the proposed sensor based on the structure-switching signal-on scheme and sensor regeneration.

pulse voltammetry (DPV) measurement was carried out under the following conditions: potential range of –0.7 to 0 V *vs.* Ag/AgCl, modulation amplitude of 0.04 V, pulse width of 0.06 s, and sample width of 0.02 s.

Results and Discussion

Principle of the sensor

The proposed sensor took advantage of the high affinity of the aptamer with the target and their complex formation, which triggered the structure switching of the aptamer (Fig. 1). This structure switching decreased the distance between the redox probes labeled with the aptamer and the electrode surface, which increased the current signal. As illustrated in Fig. 1, it is simple to construct a sensing layer on the electrode surface. We used a dithiol-modified aptamer, which had no covalently labeled redox probes, unlike previous studies,[29,30] and MCH for blocking the remaining gold sites (step B). Next, MB was incubated with the aptamer modified on the electrode, and then rinsed (step C). Subsequently, MB was noncovalently labeled with the aptamer through an interaction with guanin bases, as described above. The labeled MB molecules were placed in proximity with the electrode surface and still provided low electron transfer efficiency, whose condition was referred from the background of the current signal. The addition of the target to the sensor induced the formation of G-quadruplex conformation, resulting in structural switching of the aptamer.[31] Furthermore, the MB molecule became closer to the electrode surface, generating a higher current than the background (step D). After the analysis, the sensing layer of the sensor was regenerated as described below.

Sensing layer modification with aptamer, MB, and MCH

In this study, the aptamer was directly immobilized onto a gold surface with a dithiol-based anchor by chemisorption. We previously reported a DNA aptamer sensor in which the aptamer was immobilized with a monothiol-based linker having a sequence that hybridized with part of the aptamer.[11] As described above, several studies have revealed that MCH displaced the thiol compound originally immobilized on the electrode[25] while it was required for filling the remaining gold

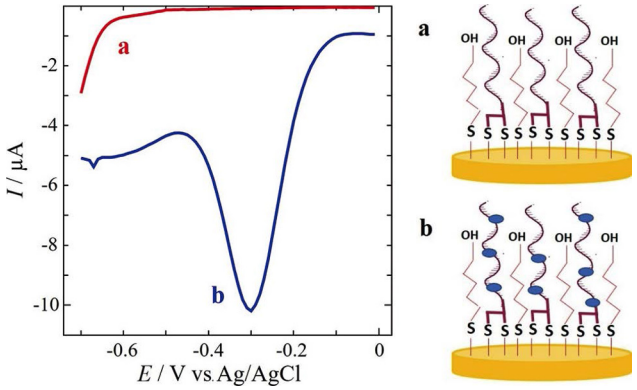

Fig. 2 Current responses obtained before and after electrode modification: a) aptamer- and MCH-modified electrode and b) MB-modified electrode. These responses were obtained in PBS containing 1 mM $MgCl_2$.

site of the sensing layer. This displacement frequently occurred for a mono-thiol-anchored aptamer, which has a similar binding energy of 30 – 45 kcal/mol to MCH.[25] Thus, the stable anchoring of the aptamer is crucial for reproducible sensor signals; here, we used an aptamer that had two thiol groups to obtain a more stable immobilization of the aptamer (Fig. S3, Supporting Information).

The modification of the electrode was electrochemically monitored in a stepwise manner with DPV in PBS containing 1 mM $MgCl_2$. As shown in Fig. 2, immobilizing the aptamer and MCH provided no peak current (curve a), indicating that the electrode surface was fully covered with these compounds. Afterward, the electrode was incubated in an MB solution for 10 min and rinsed with PBS buffer. The MB-modified electrode exhibited a peak current at a potential of –0.3 V *vs.* Ag/AgCl (curve b). This peak current was attributed to the remaining MB interacted with the aptamer immobilized on the electrode surface. The MB molecules specifically bind only with guanine bases through electrostatic interaction. Similar results were revealed in previous research.[18–20,27]

The stability of the dithiol-modified aptamer immobilized on the gold surface was tested by measuring the DPV responses

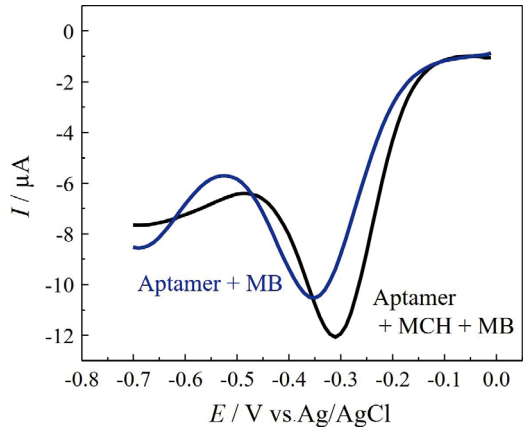

Fig. 3 Effect of addition of MCH to the dithiol modified aptamer on the electrode surface.

with two electrodes that were treated with and without MCH. Figure 3 shows that similar peak currents (differences between the peak top and baseline) were obtained with and without MCH. This result indicates that the dithiol-modified aptamer was not replaced with MCH. However, the peak potential shifted by approximately 0.05 V by adding MCH, which could be due to the difference in the coverage of thiol compounds over the electrode surfaces.

We also examined the reproducibility of sensor modification with the aptamer and MCH using six different electrodes. As shown in Fig. S2, the sensors provided an almost constant peak current with the coefficient of variation of 5.9% after immobilization with the aptamer and MCH, followed by incubation with MB. This result confirmed that the immobilization of the aptamer and MCH was conducted reproducibly.

Characterization of the sensor

The above-mentioned electrode-modification scheme was examined at various concentrations of OTA. As shown in Fig. 4A, the sensor offered a peak current around –0.3 V *vs.* Ag/AgCl, and increasing the concentration of OTA increased the peak current. The peak current reached a plateau at the OTA concentration above 750 nM (data not shown), which indicated that the aptamer was saturated with OTA. Figure 4B displays a linear relation between the peak current and the logarithm of the concentration in the OTA concentration range of 0.25 – 750 nM with a coefficient of correlation of 0.990. The limit of detection was 113 pM (45 pg mL^{-1}). This value satisfied the required minimum amount of OTA considered safe for human consumption (2 – 10 ng mL^{-1}).

Next, to characterize the affinity of the dithiol-modified aptamer with OTA, we determined the dissociation constant of the aptamer-OTA complex. We assumed a negligible intermolecular interaction among aptamers with equal binding energy and uniform binding sites on the surface of the gold electrode. The equilibrium and dissociation constants can be written as follows:

$$A + T \rightleftharpoons C \quad (1)$$

$$K_d = \frac{[A][T]}{[C]} \quad (2)$$

where [A], [T], [C], and K_d indicate the free aptamer

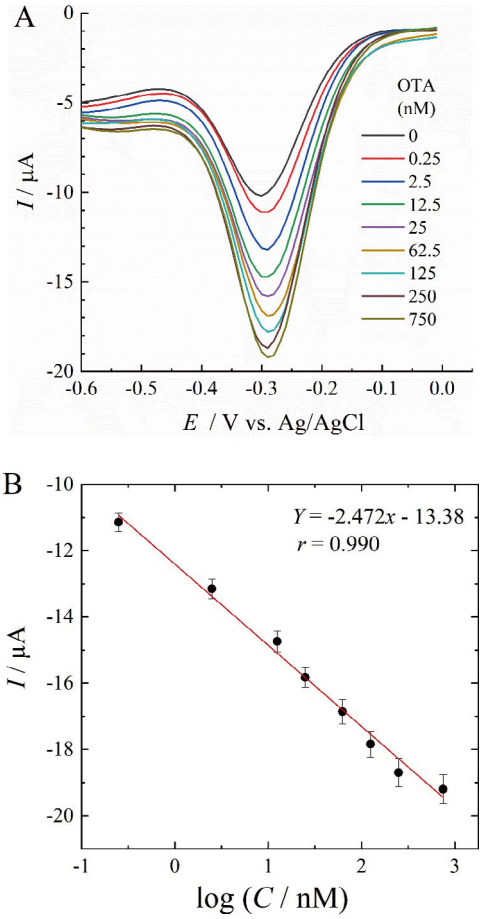

Fig. 4 (A) DPV signal currents in response to various OTA concentrations. (B) Logarithmic dependences of current responses upon the OTA concentration. All data points are presented as the mean ± standard deviation (n = 3).

concentration on the electrode surface, free OTA concentration in solution, the concentration of the aptamer-target complex at the electrode, and the dissociation constant, respectively. Equation (3) can be derived from Eq. (2) with Eqs. (4) and (5), as follows:[28,32]

$$\frac{[C]}{[A]_T} = \frac{[T]_T + K_d + [A]_T - \sqrt{[T]_T^2 + (2K_d - 2[A]_T)[T]_T + K_d^2 + 2[A]_T K_d + [A]_T^2}}{2[A]_T}, \quad (3)$$

$$[A]_T = [A] + [C], \quad (4)$$

$$[T]_T = [T] + [C] \quad (5)$$

where $[A]_T$ and $[T]_T$ are the total concentrations of the aptamer and OTA, respectively. We also assume that the net peak current (the difference in the peak current between) at a given total concentration of OTA is proportional to the concentration of the complex, as expressed by

$$I - I_0 \propto [C] \quad (6)$$

where I and I_0 are the peak currents obtained at $[T]_T$ and $[T]_T = 0$, respectively. In addition, when the peak current reached a plateau, the following equation is obtained by supposing $[C] \approx [A]_T$,

$$I_{max} - I_0 \propto [A]_T \quad (7)$$

Thus, the fraction of the complex concentration on the surface to total aptamer concentration, $[C]/[A]_T$, can be obtained by

$$\frac{[C]}{[A]_T} = \frac{I - I_0}{I_{max} - I_0} \quad (8)$$

The K_d value was determined by fitting the experimental data (plot of $I - I_0$ *vs.* $[T]_T$) to Eq. (8) by using the nonlinear regression method and OriginPro 2019 software (Massachusetts, USA) (Fig. S4, Supporting Information). The dissociation constant (K_d) was 12.6 nM. This value was close to the value previously published for an electrochemical aptamer sensor for OTA (~9 nM),[32] while it was one order of magnitude smaller than the values obtained by Cruz-Aguado and Penner, and Zhao *et al*.[28,33] The discrepancy was due to immobilization of the aptamer and differences in detection schemes and experimental conditions.

Selectivity test with mycotoxins

Many fungi produce more than one mycotoxin under similar environmental conditions, and therefore, the sensor must have specificity to the target mycotoxin to avoid false-positive result. AFB1 and DON are the most common toxins found with OTA. These mycotoxins have molecular weight and functional groups similar to those of groups such as phenyl, hydroxyl, and methyl. To evaluate the specificity of the proposed sensor, the proposed sensor was exposed to separately prepared solutions and the mixture of the mycotoxins, and then the DPV currents were measured at a potential of –0.3 V *vs.* Ag/AgCl. As shown in Fig. 5, a less significant increase in the current was observed for each AFB1 and DON solution, while the current significantly increased in the OTA solution. A similar current signal was observed with a mixture of AFB1, DON, and OTA, each with a concentration of 250 nM. These results indicate that the proposed sensor had a high specificity to OTA against other mycotoxins.

Regeneration of sensing layer

Reusability is another advantage of the electrochemical aptasensor. In this study, the proposed sensor was regenerated, as shown in the Experimental section. Briefly, the sensor was incubated with 50 mM NaOH, which is an efficient denaturant reagent for the aptamer[34] and disturbs the interaction between the aptamer and OTA by shifting the pH. Denaturation promoted OTA release without affecting the affinity of the surface-bound aptamer. Furthermore, the aptamer was renatured with PBS buffer and incubated again with an MB solution (Fig. 1). Figure S5 (Supporting Information) shows the currents measured without and with 250 nM OTA after sensor regeneration. Repeating six regenerations offered a constant current with the coefficient of variation of 3.7%, indicating that the aptamer still remains on the surface of the electrode after at least five regenerations. This suggested a high stability of the dithiol-modified aptamer immobilized on the electrode surface. However, when the sensor was regenerated for more than five times, the counter-electrode was damaged, as shown in Fig. S6 (Supporting Information), and the current considerably decreased, as shown in Table S1 (Supporting Information). This remains a challenge for the microfabricated thin film and an opportunity for improvement in the future.

Comparison of the performance of the proposed sensor with other aptasensors

The performances of the aptamer-based sensors, including the proposed sensor, are summarized in Table 1. The proposed sensor offered a higher limit of detection than the sensors presented previously. However, as mentioned above, it has achieved the practically required sensitivity for detection of the minimum amount of OTA (2 – 10 ng mL^{-1}) without signal amplification.

Although most of the electrochemical sensors developed previously focused on lower detection limits and wider linear range of detection, only a few studies have discussed the stability of the sensing layer. Note that the stability of the

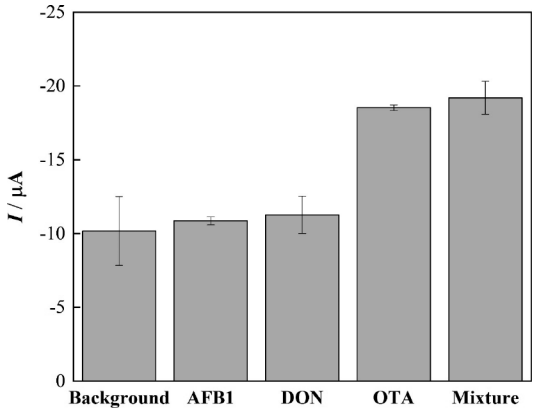

Fig. 5 Selectivity of the proposed sensor toward OTA. The concentrations of AFB1, DON, and OTA were 250 nM in this experiment and the background corresponding to the signal current without mycotoxin. The mixture contains AFB1, DON, and OTA. All bars are presented as the mean ± standard deviation (n = 3).

Table 1 Performance comparisons of electrochemical aptasensor for OTA detection

Platform	Detection limit/pg mL^{-1}	Linear range/g mL^{-1}	Reproducibility, CV%	Label/probe	Signal amplifier	Ref.
SPCE modified with thionine	5.6	0.004 - 40	N/A	Label-free/Impedance	IrO_2NPs	10
Conventional electrode	0.005	5×10^{-6} - 5×10^{-4}	N/A	Label-free/MB	AuNPs	14
Conventional electrode	1	0.005 - 10	N/A	Covalently labeled ferrocene	Exonuclease	16
Conventional electrode	21	N/A	N/A	Covalently labeled MB	SWCNTs	23
Fe_3O_4 Au magnetic beads	5.4	0.015 -100	5.3	Covalently labeled fluorescence	HFNPs quantum dots	24
Microfabricated electrode	45	0.1 - 300	5.9	Label-free/MB	Not used	This work

SPCE: Screen-printed carbon electrode. IrO_2NPs: Iridium oxide nanoparticles. MB: Methylene blue. SWCNTs: Single-walled carbon nanotubes. HFNPs: Hybrid fluorescent nanoparticles. N/A: Not available. The data were not provided in the paper.

immobilized aptamer in the electrode is very important to provide reproducible results and avoid biased results. The proposed sensor demonstrated advantages of simple fabrication and good reproducibility with DTPA-modified aptamer in the microfabricated system. The present scheme for immobilization of the dithiol-modified aptamer can be applied to various platforms for sensors that require stable anchoring of the aptamer with Au materials, such as screen-printing gold electrodes and carbon nanotubes with gold nanoparticles. In addition, the reagent consumption involved in this study was very small (50 μL) compared to the conventional ones (at least 2 mL).

Conclusions

Herein, a signal-on microfabricated electrochemical sensor based on the target-induced structure switching of the dithiol-modified aptamer was developed. We used the end-site modification of the aptamer with dithiol as the anchor site, which provided good stability and reproducibility of the sensing layer after adding the monothiol blocking agent, MCH. We also employed a non-covalent labeled probe, MB, which interacted with the aptamer and generated a stable redox signal without a specific signal enhancer. The proposed modification scheme for the aptamer was successively applied to the microfabricated electrode. The sensor exhibited quantitative responses to a wide concentration range of OTA and provided good linearity in their standard curve. The proposed sensor also provided good selectivity and reusability. Moreover, this characteristic offered a potential tool for simple and portable on-site detection for the universal platform by changing the corresponding aptamer. Future research will be directed to the extension of the stability of the immobilized aptamer by modifying the anchoring group with triple DTPA, and then integrating it into a microfluidic device.

Acknowledgements

A part of this study was supported by the Hokkaido University microstructural characterization platform as a program of "Nanotechnology Platform" of the Ministry of Education, Culture, Sports, Science and Technology (MEXT), Japan. D. N. M. thanks the international educational program "Advanced Graduate School of Chemistry and Materials Science (AGS)" of the Graduate School of Chemical Sciences and Engineering, Hokkaido University.

Supporting Information

The microfabricated three-electrode system and technique for electrochemical experiments. The electrochemical system used in this study. The currents after incubating with MB on six separately fabricated sensors. Fraction of complex concentration to total aptamer concentration as a function of the OTA concentration for the determination of the dissociation constant (K_d) of the aptamer-OTA complex. The microfabricated electrodes used in this experiment. The peak currents after regeneration of microfabricated electrochemical aptasensor. This material is available free of charge on the Web at http://www.jsac.or.jp/analsci/.

References

1. R. Remiro, M. Ibáñez-Vea, E. González-Peñas, and E. Lizarraga, *J. Chromatogr. A*, **2010**, *1217*, 8249.
2. D. Kwon, J. Joo, J. Lee, K. H. Park, and S. Jeon, *Anal. Chem.*, **2013**, *85*, 7594.
3. D. Schiff, H. Aviv, E. Rosenbaum, and Y. R. Tischler, *Anal. Chem.*, **2016**, *88*, 2164.
4. Z. Hruska, H. Yao, R. Kincaid, R. Brown, T. Cleveland, and D. Bhatnagar, *Food Bioprocess Technol.*, **2014**, *7*, 1195.
5. V. C. Ozalp, G. Bayramoglu, Z. Erdem, and M. Y. Arica, *Anal. Chim. Acta*, **2015**, *853*, 533.
6. A. Fulgione, M. Cimafonte, B. Della Ventura, M. Iannaccone, C. Ambrosino, F. Capuano, Y. T. R. Proroga, R. Velotta, and R. Capparelli, *Sci. Rep.*, **2018**, *8*, 1.
7. P. Wang, X. Hu, Q. Cheng, X. Zhao, X. Fu, and K. Wu, *J. Agric. Food Chem.*, **2010**, *58*, 12112.
8. N. Y. Jayanath, L. T. Nguyen, T. T. Vu, and L. D. Tran, *RSC Adv.*, **2018**, *8*, 34954.
9. Nandakumar, D. Bishop, E. Alonas, J. LaBelle, L. Joshi, and T. L. Alford, *IEEE Sens. J.*, **2011**, *11*, 210.
10. L. Rivas, C. C. Mayorga-Martinez, D. Quesada-González, A. Zamora-Gálvez, A. De La Escosura-Muñiz, and A. Merkoçi, *Anal. Chem.*, **2015**, *87*, 5167.
11. D. N. Mazaafrianto, A. Ishida, M. Maeki, H. Tani, and M. Tokeshi, *ACS Omega*, **2018**, *3*, 16823.
12. S. D. Jayasena, *Clin. Chem.*, **1999**, *45*, 1628.
13. D. Irvine, C. Tuerk, and L. Gold, *J. Mol. Biol.*, **1991**, *222*, 739.
14. M. Wei and S. Feng, *Anal. Methods*, **2017**, *9*, 5449.
15. J. Zhang, Y. K. Xia, M. Chen, D. Z. Wu, S.X. Cai, M. M. Liu, W. H. He, and J. H. Chen, *Sens. Actuators, B*, **2016**, *235*, 79.
16. P. Tong, L. Zhang, J. J. Xu, and H. Y. Chen, *Biosens. Bioelectron.*, **2011**, *29*, 97.
17. E. Gonzalez-Fernandez, N. Avlonitis, A. F. Murray, A. R. Mount, and M. Bradley, *Biosens. Bioelectron.*, **2015**, *84*, 82.
18. E. Doğru, E. Erhan, and O. A. Arikan, *Int. J. Electrochem. Sci.*, **2016**, *11*, 829.
19. W. Yang, M. Ozsoz, D. B. Hibbert, and J. J. Gooding, *Electroanalysis*, **2002**, *14*, 1299.
20. C. G. Pheeney and J. K. Barton, *Langmuir*, **2012**, *28*, 7063.
21. X. Lin, Y. Ni, and S. Kokot, *Anal. Chim. Acta*, **2015**, *867*, 29.
22. E. Papadopoulou, N. Gale, J. F. Thompson, T. A. Fleming, T. Brown, and P. N. Bartlett, *Chem. Sci.*, **2015**, *7*, 386.
23. K. Abnous, N. M. Danesh, M. Alibolandi, M. Ramezani, and S. M. Taghdisi, *Microchim. Acta*, **2017**, *184*, 1151.
24. C. Wang, J. Qian, K. Wang, K. Wang, Q. Liu, X. Dong, C. Wang, and X. Huang, *Biosens. Bioelectron.*, **2015**, *68*, 783.
25. P. Liepold, T. Kratzmüller, N. Persike, M. Bandilla, M. Hinz, H. Wieder, H. Hillebrandt, E. Ferrer, and G. Hartwich, *Anal. Bioanal. Chem.*, **2008**, *391*, 1759.
26. N. Garg, A. Mohanty, N. Lazarus, L. Schultz, T. R. Rozzi, S. Santhanam, L. Weiss, J. L. Snyder, G. K. Fedder, and R. Jin, *Nanotechnology*, **2010**, *21*, 1.
27. E. Papadopoulou, N. Gale, J. F. Thompson, T. A. Fleming, T. Brown, and P. N. Bartlett, *Chem. Sci.*, **2015**, *7*, 386.
28. J. A. Cruz-Aguado and G. Penner, *J. Agric. Food Chem.*, **2008**, *56*, 10456.
29. J. Chen, Z. Fang, J. Liu, and L. Zeng, *Food Control*, **2012**, *25*, 555.
30. Y. Xiao, R. Y. Lai, and K. W. Plaxco, *Nat. Protoc.*, **2007**, *2*, 2875.
31. K. L. Fadock and R. A. Manderville, *ACS Omega*, **2017**, *2*, 4955.
32. H. Kuang, W. Chen, D. Xu, L. Xu, Y. Zhu, L. Liu, H. Chu, C. Peng, C. Xu, and S. Zhu, *Biosens. Bioelectron.*, **2010**, *26*, 710.
33. Q. Zhao, X. Geng, and H. Wang, *Anal. Bioanal. Chem.*, **2013**, *405*, 6281.
34. K. Lee, J. Ahn, S. Lee, S. S. Sekhon, D. Kim, J. Min, and Y. Kim, *Sci. Rep.*, **2015**, *5*, 10897.